crystallization communications

Jian Gao,[a]‡ Yuanyuan Ma,[b]‡ Yuna Sun,[c] Huadong Zhao,[d] Dapeng Hong,[e] Liming Yan[a]* and Zhiyong Lou[a]*

[a]Laboratory of Structural Biology, School of Medicine, Tsinghua University, Beijing 100084, People's Republic of China, [b]College of Life Science, Nankai University, Tianjin 300074, People's Republic of China, [c]National Laboratory of Macromolecules, Institute of Biophysics, Chinese Academy of Science, Beijing 100101, People's Republic of China, [d]High-throughput Molecular Drug Discovery Center, Tianjin Joint Academy of Biotechnology and Medicine, Tianjin 300071, People's Republic of China, and [e]High School Attached to Capital Normal University, Beijing, People's Republic of China

‡ These authors contributed equally.

Correspondence e-mail:
yanlm@xtal.tsinghua.edu.cn,
louzy@xtal.tsinghua.edu.cn

Crystallization and preliminary crystallographic analysis of *Arabidopsis thaliana* BRI1-associated kinase 1 (BAK1) cytoplasmic domain

BRI1-associated kinase 1 (BAK1) is a member of the plant receptor-like kinase (RLK) superfamily. BAK1 has been shown to initiate brassinosteroid (BR) signalling and innate immune responses in plants by forming receptor complexes with both brassinosteroid-insensitive 1 (BRI1) and flagellin-sensing 2 (FLS2). To gain a better understanding of the structural details and the mechanism of action of the BAK1 kinase domain, recombinant BAK1 cytoplasmic domain has been expressed, purified and crystallized at 291 K using PEG 3350 as a precipitant. A 2.6 Å resolution data set was collected from a single flash-cooled crystal at 100 K. This crystal belonged to space group $C2$, with unit-cell parameters $a = 70.3$, $b = 75.6$, $c = 71.9$ Å, $\beta = 93.1°$. Assuming the presence of one molecule in the asymmetric unit, the Matthews coefficient was 2.6 $Å^3\,Da^{-1}$.

1. Introduction

Receptor-like kinases (RLKs) constitute the major superfamily of cell-surface-associated receptors in plant cells and play essential roles in perceiving external stimuli and transducing the extracellular signals to transcriptional programmes (Zipfel, 2008; Tang *et al.*, 2010). The structurally related RLK-family members share similarities with tyrosine and serine/threonine kinases and normally have an extracellular domain for ligand binding, a single transmembrane helix and a cytoplasmic portion (CD) containing a kinase domain (KD) that catalyses phosphoryl transfer from ATP to residues in protein substrates and initiates intracellular signal transduction. In addition to their roles in plant immunity (Gao *et al.*, 2011; Gómez-Gómez & Boller, 2000; Han *et al.*, 2011; Ho *et al.*, 2010; Liu *et al.*, 2011; Tena *et al.*, 2011; Zipfel *et al.*, 2006), RLKs play essential roles in core cellular processes in plant cells, including cell and organ elongation (van Zanten *et al.*, 2009; Brutus *et al.*, 2010), floral organ abscission (Lewis *et al.*, 2011), maintenance of the apical meristem (Fletcher *et al.*, 1999; Brand *et al.*, 2000), epidermal cell specification (Stokes & Gururaj Rao, 2008) and brassinosteroid signalling (Nam & Li, 2002).

BRI1-associated kinase 1 (BAK1) is one of the best-studied leucine-rich repeat RLKs (LRR-RLKs) among hundreds of members of this family in *Arabidopsis*. BAK1 was initially identified based on its association with brassinosteroid-insensitive 1 (BRI1), the receptor of brassinosteroids (BRs), which regulates a wide range of developmental and physiological processes in plants (Tang *et al.*, 2010). BAK1 mediates BRI1 function *in vivo* through sequential phosphorylation of specific residues in the cytoplasmic domain of BRI1, thereby increasing BRI1 kinase activity and enhancing BR signal transduction. In addition to its critical role in BR signalling for plant growth, BAK1 has recently been discovered to impact plant MAMP/PAMP-triggered immunity (PTI) through the formation of heterodimers with other pattern-recognition receptors (PRRs) such as flagellin-sensing 2 (FLS2) in a BR-independent manner (Chinchilla *et al.*, 2007; Heese *et al.*, 2007; Zipfel *et al.*, 2006). Therefore, BAK1 plays key roles in multiple independent pathways by enhancing the signalling output of distinct LRR-RLKs that bind different ligands (Zipfel *et al.*, 2006; Heese *et al.*, 2007; Shan *et al.*, 2008).

The earliest signalling events following BR binding to BRI1 or flg22 binding to FLS2 involve the robust association of BAK1 with
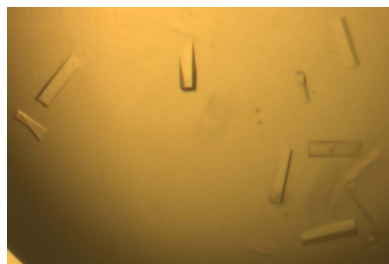
specific LRR-RLKs on the cell surface, followed by rapid trans-phosphorylation within the kinase pair. The reciprocal phosphorylation of the cytosolic domains of BAK1 and BRI1 in the complex is a prerequisite for the full expression of BAK1-mediated signalling cascades (Chinchilla *et al.*, 2007). However, it is still not clear how phosphorylation activates BAK1 kinase activity at the molecular level. To gain a better understanding of the structural basis of the activation of BAK1 kinase activity, we report the crystallization and preliminary crystallographic studies of the cytoplasmic domain of BAK1 (BAK1-CD).

2. Protein expression and purification

The primers 5′-CGC **GGA TCC** ATG TTT GAT GTA CCA GCT GAA GAG G-3′ and 5′-CCG **CTC GAG** TCA TTG TCT GAA CAT TTC CTC CTT TTG-3′ were used to amplify the BAK1-CD gene from an in-house *A. thaliana* Col-0 cDNA library. The primers included *Bam*HI and *Xho*I restriction sites (shown in bold). The PCR conditions were as follows: 1 min at 367 K, 1 min at 328 K and 2 min at 345 K for 30 cycles. The purified PCR products were digested by *Bam*HI and *Xho*I and then inserted into the expression vector pET-28b-SUMO with the same digested sites. After transformation into *Escherichia coli* Top10, the cloned fragments were completely sequenced. The recombinant plasmid was transformed into *E. coli* strain BL21 (DE3). The transformed cells were cultured at 310 K in LB medium containing 100 mg l^{-1} kanamycin. After the OD$_{600}$ had reached 0.8, the culture was cooled to 289 K and supplemented with 0.5 mM IPTG. After overnight induction, the cells were harvested by centrifugation and the pellets were resuspended in lysis buffer consisting of 20 mM Tris–HCl pH 8.0, 150 mM NaCl, 4 mM MgCl$_2$ and homogenized with an ultrahigh-pressure cell disrupter (JNBIO) at 277 K. Insoluble material was removed by centrifugation at 12 000 rev min^{-1}. The fusion protein was first purified by Ni–NTA affinity chromatography (1.5 ml Ni^{2+}–NTA agarose, Qiagen, USA) and eluted with lysis buffer with an additional 200 mM imidazole. Ulp1 protease was subsequently added to a final concentration of 0.05 mM for 12 h at 289 K to remove the 6×His-SUMO tag and the protein was then further purified by passage through a Mono-Q ion-exchange column (GE Healthcare) using a 0–1 M NaCl gradient in 20 mM Tris–HCl pH 8.0 buffer. The purity of the target BAK1-CD protein was estimated to be greater than 99% by SDS–PAGE and the purified BAK1-CD was concentrated to 20 mg ml^{-1} and stored at 193 K.
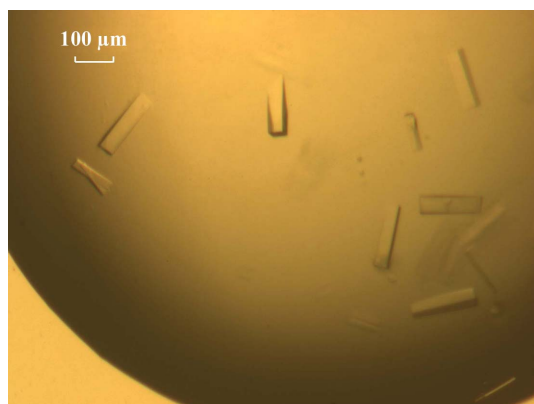

Figure 1
Crystals of BAK1 cytoplasmic domain grown in 21% PEG 3350, 200 mM sodium citrate, 50 mM ammonium sulfate, 20 mM HEPES pH 7.5.

Table 1
Data-collection and processing statistics for apo BAK1-CD.

Values in parentheses are for the highest resolution shell.

Unit-cell parameters	
a (Å)	70.3
b (Å)	75.6
c (Å)	71.9
α (°)	90.0
β (°)	93.1
γ (°)	90.0
Space group	$C2$
Wavelength used (Å)	1.0000
Resolution (Å)	50.00–2.60 (2.69–2.60)
Total No. of reflections	55664 (4920)
No. of unique reflections	11442 (1046)
Completeness (%)	97.1 (90.2)
Average $I/\sigma(I)$	15.6 (4.6)
R_{merge}† (%)	5.8 (31.6)

† $R_{merge} = \sum_{hkl} \sum_i |I_i(hkl) - \langle I(hkl)\rangle| / \sum_{hkl} \sum_i I_i(hkl)$, where $\langle I(hkl)\rangle$ is the mean of the observations $I_i(hkl)$ of reflection hkl.

3. Crystallization

Crystallization was performed at 291 K using the hanging-drop vapour-diffusion technique. Crystals were obtained by mixing 1 µl protein solution with an equal volume of reservoir solution and equilibrating against 500 µl reservoir solution. Initial trials were carried out using commercial crystallization screens (Crystal Screen and Crystal Screen 2; Hampton Research), which failed to produce suitable crystals. However, solutions containing polyethylene glycol (PEG) 4000 produced a granular precipitate. Further trials for screening and optimization were carried out using the PEG/Ion kit (Hampton Research). Microcrystals appeared after 5 d in 20% PEG 3350, 200 mM sodium citrate, 50 mM ammonium sulfate, 20 mM HEPES pH 7.5. After several rounds of optimization, which included changing variables such as temperature, pH, protein concentration, PEG 3350 concentration and ammonium sulfate concentration in 160 droplets, rectangular-shaped crystals with good diffraction quality were obtained from 21% PEG 3350, 200 mM sodium citrate, 50 mM ammonium sulfate, 20 mM HEPES pH 7.5 and reached final dimensions of 50 × 50 × 200 µm after 7 d (Fig. 1). Additive screens and detergent screens from Hampton Research were used to gauge their effect on crystal quality, but no significant effects could be observed.

4. X-ray diffraction analysis

The crystal was mounted on a nylon loop and flash-cooled in a nitrogen-gas cryostream (Oxford Cryosystems) at 100 K. We tested various cryoprotectants (*e.g.* PEG 400, glycerol, sugar, oil *etc.*) and tried different methods of introducing the cryoprotectant into the crystal. However, all attempts led to destruction of the apo BAK1-CD crystal. We resorted to using the native conditions and cryo-mounting the crystals directly from the drop; only slight ice rings could be observed in the final diffraction patterns.

Native diffraction data for BAK1-CD were collected at 100 K using a MAR 165 CCD detector (MAR Research, Hamburg) on beamline 1W2A at Beijing Synchrotron Radiation Facility (BSRF). A total of 540 frames of data were collected with 0.5° oscillation range (Fig. 2). All intensity data were indexed, integrated and scaled with the *HKL*-2000 package (Otwinowski & Minor, 1997). The crystal belonged to space group $C2$, with unit-cell parameters a = 70.3, b = 75.6, c = 71.9 Å, $\alpha = \gamma = 90$, $\beta = 93.1°$. We assumed the presence of one molecule per asymmetric unit, which gives a Matthews coefficient of 2.6 Å^3 Da^{-1} and 47% solvent content (Matthews, 1968).
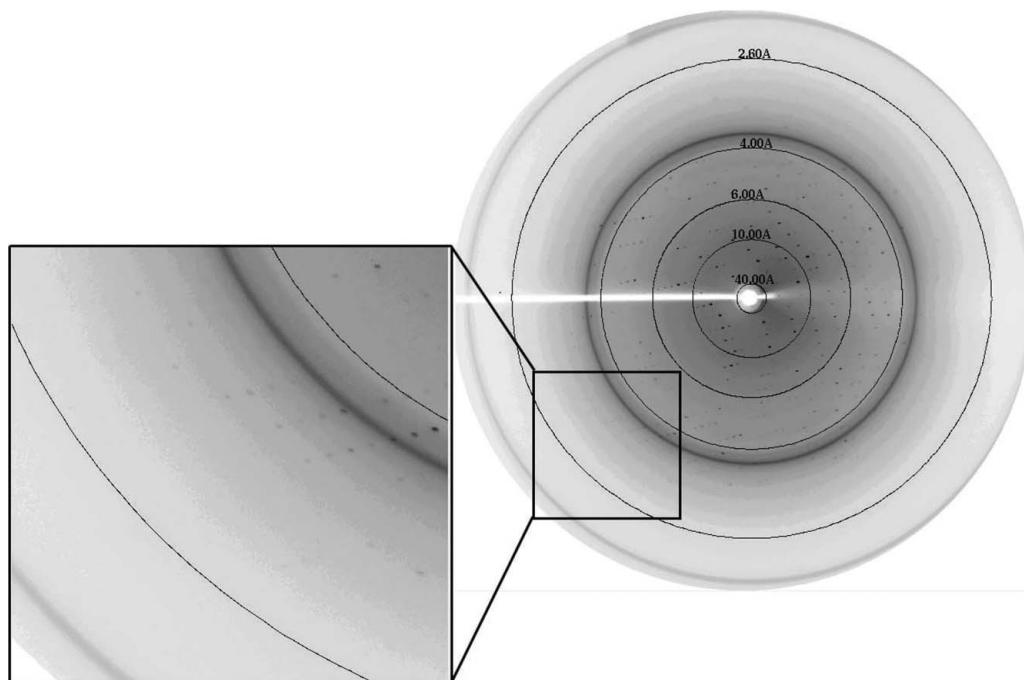
Figure 2
A typical diffraction pattern of a crystal of the BAK1 cytoplasmic domain. The exposure time was 30 s, the crystal-to-detector distance was 164 mm and the oscillation range per frame was 0.5° at a wavelength of 1.0000 Å. The diffraction images were collected on a MAR 165 CCD detector.

Since the members of the kinase superfamily usually share relatively high structural similarity, molecular replacement (MR) was performed using the crystal structure of IRAK-4 kinase (PDB entry 2nry; Wang *et al.*, 2006), which shows 33% sequence identity to BAK1-CD, as the initial search model. Clear rotation-function and translation-function pairs were obtained using *Phaser* (McCoy *et al.*, 2007) and suggested the correct MR solution. Further structure refinement and soaking with ATP analogues to obtain complex structures is currently under way. The final statistics of data collection and processing are summarized in Table 1.

References

Brand, U., Fletcher, J. C., Hobe, M., Meyerowitz, E. M. & Simon, R. (2000). *Science*, **289**, 617–619.
Brutus, A., Sicilia, F., Macone, A., Cervone, F. & De Lorenzo, G. (2010). *Proc. Natl Acad. Sci. USA*, **107**, 9452–9457.
Chinchilla, D., Zipfel, C., Robatzek, S., Kemmerling, B., Nürnberger, T., Jones, J. D., Felix, G. & Boller, T. (2007). *Nature (London)*, **448**, 497–500.
Fletcher, J. C., Brand, U., Running, M. P., Simon, R. & Meyerowitz, E. M. (1999). *Science*, **283**, 1911–1914.
Gao, L., Zhang, W. & Chen, W. (2011). *Acta Biophys. Sin.* **27**, 676–686.
Gómez-Gómez, L. & Boller, T. (2000). *Mol. Cell*, **5**, 1003–1011.
Han, S., Yu, B., Wang, Y. & Liu, Y. (2011). *Protein Cell*, **2**, 784–791.
Heese, A., Hann, D. R., Gimenez-Ibanez, S., Jones, A. M., He, K., Li, J., Schroeder, J. I., Peck, S. C. & Rathjen, J. P. (2007). *Proc. Natl Acad. Sci. USA*, **104**, 12217–12222.
Ho, T., Wang, L., Huang, L., Li, Z., Pallett, D. W., Dalmay, T., Ohshima, K., Walsh, J. A. & Wang, H. (2010). *Protein Cell*, **1**, 847–858.
Lewis, M. W., Leslie, M. E., Fulcher, E. H., Darnielle, L., Healy, P. N., Youn, J.-Y. & Liljegren, S. J. (2011). *Plant J.* **62**, 817–828.
Liu, Y., Dong, J. & Chen, W. (2011). *Acta Biophys. Sin.* **27**, 517–527.
Matthews, B. W. (1968). *J. Mol. Biol.* **33**, 491–497.
McCoy, A. J., Grosse-Kunstleve, R. W., Adams, P. D., Winn, M. D., Storoni, L. C. & Read, R. J. (2007). *J. Appl. Cryst.* **40**, 658–674.
Nam, K. H. & Li, J. (2002). *Cell*, **110**, 203–212.
Otwinowski, Z. & Minor, W. (1997). *Methods Enzymol.* **276**, 307–326.
Shan, L., He, P., Li, J., Heese, A., Peck, S. C., Nürnberger, T., Martin, G. B. & Sheen, J. (2008). *Cell Host Microbe*, **4**, 17–27.
Stokes, K. D. & Gururaj Rao, A. (2008). *Arch. Biochem. Biophys.* **477**, 219–226.
Tang, W., Deng, Z. & Wang, Z.-Y. (2010). *Curr. Opin. Plant Biol.* **13**, 27–33.
Tena, G., Boudsocq, M. & Sheen, J. (2011). *Curr. Opin. Plant Biol.* **14**, 519–529.
Wang, Z., Liu, J., Sudom, A., Ayres, M., Li, S., Wesche, H., Powers, J. P. & Walker, N. P. (2006). *Structure*, **14**, 1835–1844.
Zanten, M. van, Snoek, L. B., Proveniers, M. C. & Peeters, A. J. (2009). *Trends Plant Sci.* **14**, 214–218.
Zipfel, C. (2008). *Curr. Opin. Immunol.* **20**, 10–16.
Zipfel, C., Kunze, G., Chinchilla, D., Caniard, A., Jones, J. D., Boller, T. & Felix, G. (2006). *Cell*, **125**, 749–760.